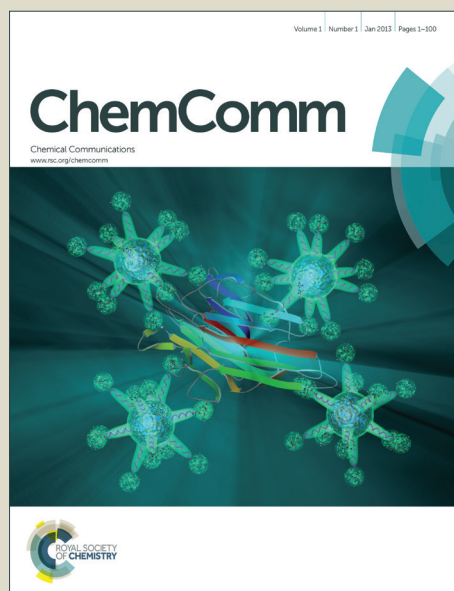


ChemComm

Accepted Manuscript



This is an *Accepted Manuscript*, which has been through the Royal Society of Chemistry peer review process and has been accepted for publication.

Accepted Manuscripts are published online shortly after acceptance, before technical editing, formatting and proof reading. Using this free service, authors can make their results available to the community, in citable form, before we publish the edited article. We will replace this *Accepted Manuscript* with the edited and formatted *Advance Article* as soon as it is available.

You can find more information about *Accepted Manuscripts* in the [Information for Authors](#).

Please note that technical editing may introduce minor changes to the text and/or graphics, which may alter content. The journal's standard [Terms & Conditions](#) and the [Ethical guidelines](#) still apply. In no event shall the Royal Society of Chemistry be held responsible for any errors or omissions in this *Accepted Manuscript* or any consequences arising from the use of any information it contains.



Journal Name

COMMUNICATION

Selective Targeting of *Mycobacterium smegmatis* with Trehalose-Functionalized Nanoparticles

Received 00th January 20xx,
Accepted 00th January 20xx

Kalana W. Jayawardana,^a H. Surangi N. Jayawardena,^{a,b} Samurrdhi A. Wijesundera,^a Thareendra De Zoysa,^a Madanodaya Sundhoro,^a Mingdi Yan^{*,a}

DOI: 10.1039/x0xx00000x

www.rsc.org/

Silica and iron oxide nanoparticles with sizes ranging from 6–40 nm were functionalized with trehalose. The trehalose-conjugated nanoparticles showed strong interactions with *Mycobacterium smegmatis* (*M. smegmatis*) and minimal interactions with macrophage (RAW 264.7) or A549 cells. In addition, trehalose-conjugated silica nanoparticles selectively interacted with *M. smegmatis* on *M. smegmatis*-treated A549 cells, demonstrating high potential of trehalose in developing targeted therapy for treating mycobacteria infection.

With an estimated 9 million new cases each year, and 1.5 million fatalities in 2013, TB, an infectious disease caused by *Mycobacterium tuberculosis*, is among the most widespread diseases to plague mankind.¹ The resurgence of TB especially the drug-resistant TB in recent years calls for the development of new diagnostic and therapeutic strategies.² TB poses additional challenges owing to the unique structure of mycobacteria. The mycobacterial cell wall resembles that of the Gram-positive bacteria, however, it has an additional layer of lipids. This lipid-rich cell wall acts as a permeability barrier to polar molecules and controls the passage of host susceptibility components such as antimicrobial drugs into the cell.³ Relatively hydrophobic antibiotics such as rifampicin and fluoroquinolones are able to diffuse through the lipid bilayer, however, only a small number of hydrophilic antibiotics can cross the bilayer through porin channels due to low abundance of mycobacterial porins on the outer membrane.⁴

This issue can potentially be overcome by using nanomaterial-based therapeutics to deliver antimicrobial drugs. Efficient uptake of nanomaterials by the cells is the first step for the effective delivery of drugs and therapeutic agents.^{5–8} Internalization of nanoparticles by mammalian cells has been well documented, leading to the conclusion of

receptor-mediated endocytosis for the uptake of nanoparticles by mammalian cells.^{9–11} For bacterial cells, however, the general view does not support endocytosis, pinocytosis or exocytosis due to the presence of the thick peptidoglycan cell wall.^{12–14} Therefore, methods facilitating the targeting of bacterial cells are of high importance in developing effective antimicrobial nanotherapeutics.

In this work, we report a general strategy to target mycobacteria by conjugating trehalose to nanoparticles. Trehalose is a non-mammalian disaccharide and is a major component in the cytosol of both *M. smegmatis* and *M. tuberculosis*, making up 1.5%–3% of the bacterial dry weight.^{15, 16} Trehalose is also incorporated into a range of mycobacterial cell wall glycolipids (e.g. trehalose 6,6'-dimycolate),^{16, 17} which participate in cell wall associated pathogenicity of *M. tuberculosis*.¹⁸ Exogenous trehalose is transported to the mycobacterial cytoplasm through the high affinity trehalose transporter system.¹⁹ The prominence of trehalose in the cytoplasm and the role that it plays towards pathogenicity has led to drug targets that can be used to disrupt trehalose biosynthesis pathways in *M. tuberculosis*.²⁰ In the work of Davis and coworkers,²¹ trehalose labeled with a fluorescent dye was used as an imaging probe to detect *M. tuberculosis in vitro*, where the dye-trehalose conjugate was internalized by the mycobacterium bacilli through the trehalose transporter.

Nanoparticles used in this study include silane-protected iron oxide magnetic nanoparticles (MNPs), silica nanoparticles (SNPs), and fluorescein (FITC)-doped silica nanoparticles (FSNPs). MNPs were prepared by heating iron (III) acetylacetonate, 1,2-hexadecanediol, oleic acid and oleylamine in dibenzyl ether, and were silanized with 3-(trihydroxysilyl)propyl methylphosphonate, monosodium salt (phosphonate-silane) to increase the water dispersibility (Scheme S1).²² Particle sizes were measured to be 6.4 ± 0.7 nm (TEM) or 6.7 ± 0.6 nm (DLS) (Fig. S1). SNPs were synthesized using a modified Stöber method,²³ and the particle size was 42.1 ± 1.9 nm (TEM) or 44.4 ± 1.7 nm (DLS) (Fig. S2). FSNPs were prepared by co-condensing tetraethyl orthosilicate with FITC-derivatized silane,^{24, 25} and the particle size was 30.2 ± 2.1

^a Department of Chemistry, University of Massachusetts Lowell, Lowell, MA 01854. E-mail: mingdi_yan@uml.edu; Fax: +1978-934-3013; Tel: +1-978-934-3647

^b David H. Koch Institute for Integrative Cancer Research Centre, Massachusetts Institute of Technology, Cambridge, MA 02139.

† Electronic Supplementary Information (ESI) available: Experimental details on the synthesis, functionalization, TEM, DLS and TGA characterization of nanoparticles, carbohydrate density measurement, TEM sample preparation and additional TEM images, SEM images and cell viability data. See DOI: 10.1039/x0xx00000x

nm (TEM) or 32.9 ± 1.9 nm (DLS) (Fig. S3). Trehalose was conjugated to nanoparticles using the photocoupling chemistry developed in our laboratory.²⁶⁻³⁰ Nanoparticles were first functionalized with perfluorophenyl azide (PFPA) by treating SNPs or FSNPs with silane-derivatized PFPA,³¹⁻³⁴ or MNPs with a phosphate-derivatized PFPA (Scheme S1, see supporting information for details).^{35, 36} The resulting PFPA-NPs (Fig. S4) showed the asymmetric stretch of the azide ($-N_3$) at ~ 2119 cm^{-1} in the FTIR spectra (Fig. S5). Trehalose was then covalently conjugated to PFPA-NPs by irradiating the particles in the presence of an aqueous solution of trehalose (Fig. S6, Scheme S1).^{35, 37, 38} The density of trehalose conjugated on nanoparticles was determined by thermal gravimetric analysis (TGA) to be 11.5×10^{-16} , 4.1×10^{-16} , 8.7×10^{-16} $\mu\text{g}/\text{nm}^2$ for Tre-SNP, Tre-MNP and Tre-FSNP, respectively (Fig. S7, Table S1). D-Glucose (Glc), β -cyclodextrin (CD) and maltoheptaose (G7) were used as controls and were conjugated to nanoparticles following the same protocol as trehalose. The densities of these carbohydrates conjugated on nanoparticles, determined by TGA, were on the same order of magnitude as those of trehalose (Table S1).

M. smegmatis was used as the model mycobacterium³⁹⁻⁴¹ because it has been widely accepted as a mycobacterium model for the development of therapeutic drugs against TB⁴²⁻⁴⁵ and it is non-pathogenic. In the experiment, carbohydrate-conjugated nanoparticles were treated with *M. smegmatis* at 37 °C for 6 h. After excess nanoparticles were removed from the medium, the samples were examined under TEM. Results showed that nanoparticles conjugated with Tre had higher interactions with *M. smegmatis* than nanoparticles modified with G7 or CD (Fig. 1a). Particles were pressed against cell wall, creating crevices on the bacilli.

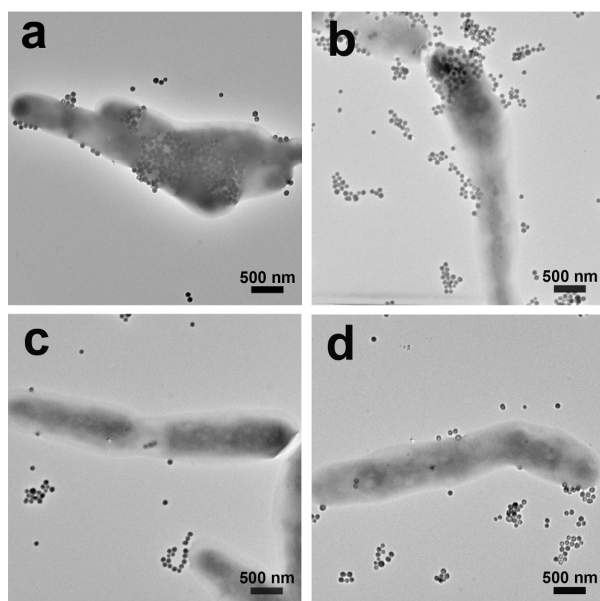


Figure 1. TEM images of *M. smegmatis* strain mc²¹⁵⁵ after incubating 6 h with (a) Tre-SNP, (b) Glc-SNPs, (c) G7-SNPs, (d) CD-SNPs.

Thin section samples prepared from the bacteria treated with Tre-MNPs showed the presence of nanoparticles at the cytoplasm of *M. smegmatis* (Fig. 2a, S8). Similar observations were obtained with nanoparticles conjugated with Glc where particles were seen on the surface (Fig. 1b) as well as inside the bacteria cells (Fig. 2b). For nanoparticles conjugated with G7 or CD, however, very little surface adherence was observed on the bacteria (Fig. 1c, 1d.). Furthermore, no particles were observed inside *M. smegmatis* from the thin section samples (Fig. 2c, 2d).

We next investigated the interactions of carbohydrate-conjugated nanoparticles with mammalian cells. In this case, FSNPs, which fluoresce green, were used to aid visualization. Tre-FSNPs were incubated with murine macrophage (RAW 264.7) in serum free DMEM medium at 37 °C for 2 h, and the sample was then treated with nucleic acid staining dye SYTO 61[®]. Laser scanning confocal microscopy (LSCM) images show that samples treated with Tre-FSNPs were mostly red, which is the color of the stained macrophages (Fig. 3a). On the other hand, samples treated with Glc-FSNPs under the same conditions appeared orange (Fig. 3b), which is the mix of red (labeled macrophages) and green (FSNPs). This demonstrates that Tre-conjugated nanoparticles had little interactions with the macrophage whereas Glc-conjugated nanoparticles interacted strongly with the macrophage. The experiment was repeated using A549 cells and Tre- or Glc-conjugated iron oxide nanoparticles. The samples were stained with potassium ferricyanide to detect the presence of iron. A549 cells treated with Tre-MNPs showed minimal color whereas cells treated with Glc-MNPs showed the typical Prussian blue color (Fig. S9). These results are consistent with those from the macrophage study that Tre-conjugated nanoparticles had little interactions with the cells whereas Glc-NPs interacted strongly with both cell lines.

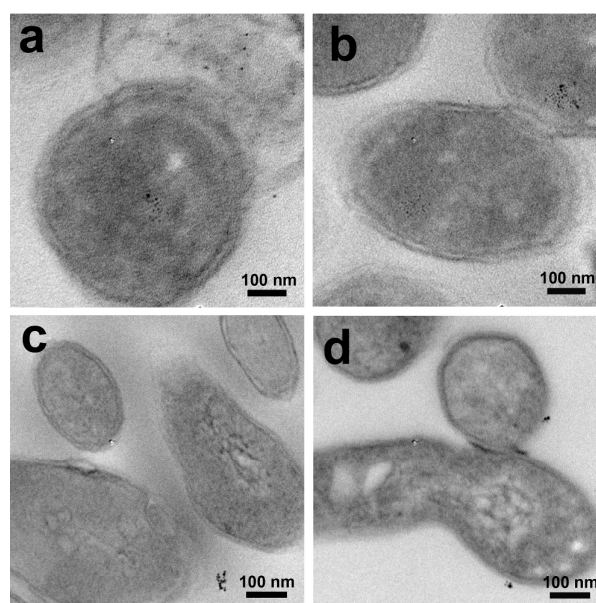


Figure 2. TEM images of thin section samples of *M. smegmatis* (mc²¹⁵⁵) after incubating 6 h with (a) Tre-MNPs, (b) Glc-MNPs, (c) G7-MNPs, (d) CD-MNPs.

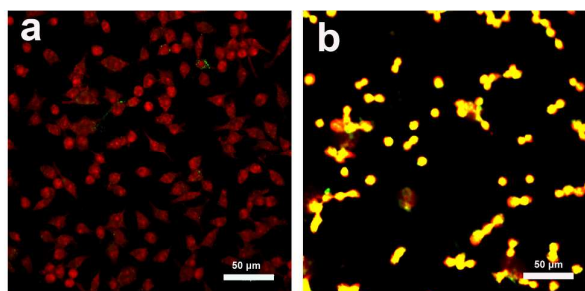


Figure 3. LSCM overlay images of murine macrophages (RAW 264.7) stained with SYTO® 61 after incubation with (a) Tre-FSNPs and (b) Glc-FSNPs.

The viability of *M. smegmatis* after treating with carbohydrate-conjugated SNPs was tested by the alamarBlue® assay. Cell viabilities of 98%, 96%, 97% and 98% were obtained for Tre-SNPs, Glc-SNPs, G7-SNPs and CD-SNPs, respectively (Fig. S10a). For A549 cells, the WST-8 assay⁴⁶ was used and cell viabilities of 99%, 99%, 78%, 98%, 98% and 85% were obtained for Tre-SNPs, Glc-SNPs, CD-SNPs, G7-SNPs, Tre-FSNPs and CD-FSNPs, respectively (Fig. S10b). These results suggest low toxicity of carbohydrate-conjugated SNPs towards the mycobacteria and A549 cells under the experimental conditions.

The selective interaction of Tre-NPs with *M. smegmatis* over mammalian cells opens up the possibility of using trehalose as the targeting ligand for mycobacteria. To further confirm the selectivity of trehalose-mediated interactions towards mycobacteria, A549 cells were treated with SYTO® 61-stained *M. smegmatis* and fixed in paraformaldehyde (5%) solution. The mycobacteria (fluoresce red) were seen on A549 cells in both (LSCM) images (Fig. 4a) and the SEM image (Fig. S11a). *M. smegmatis*-treated A549 cells were then incubated with Tre-FSNPs for 6 h. The LSCM image showed the green color (Tre-FSNPs) in the region of the A549 cells that had *M. smegmatis* (Fig. 4b). In the SEM image, nanoparticles were also observed on A549 cells where *M. smegmatis* were present (Fig. S11b). In addition, the optical image (Fig. 4c) merged with the LSCM images showed Tre-FSNPs (green) in the regions where *M. smegmatis* (red) were present (Fig. 4d). In the control experiment where the *M. smegmatis*-treated A549 cells were incubated with CD-FSNPs, no green color was seen in the LSCM image (Fig. S12) and no nanoparticles were observed on the bacteria in SEM image either (Fig. S11c). These results further supported that trehalose-mediated interactions are specific towards mycobacteria and are selective over mammalian cells.

In summary, we have demonstrated that nanoparticles conjugated with trehalose exhibits strong interactions with *M. smegmatis*. TEM thin section images revealed the presence of Tre-MNPs on the cell wall as well as in the cytoplasm of *M. smegmatis*. Furthermore, Tre-NPs had minimal interactions with macrophage (RAW 264.7) or A549 cells. When Tre-NPs were incubated with A549 cells treated with *M. smegmatis*, Tre-NPs were found only in the regions where *M. smegmatis* were present.

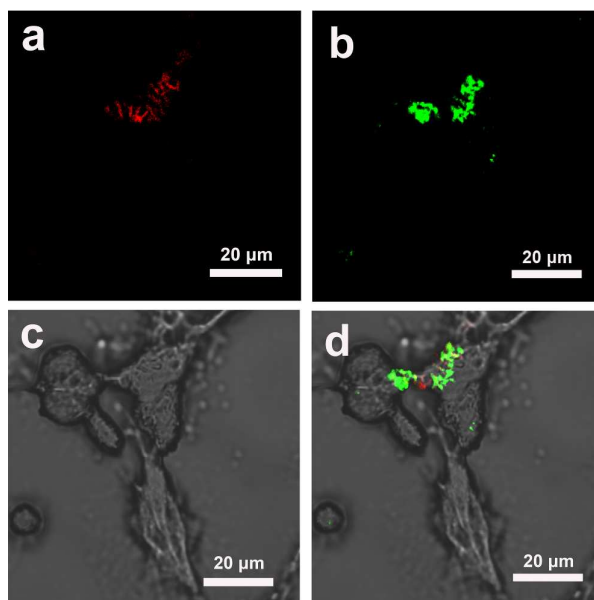


Figure 4. *M. smegmatis*-treated A549 cells incubated with Tre-FSNPs. *M. smegmatis* was stained with SYTO® 61 dye which fluoresces red. FSNPs were doped with FITC which fluoresces green. (a) LSCM image at 633 nm excitation showing SYTO® 61-stained *M. smegmatis*. (b) LSCM image at 488 nm excitation showing Tre-FSNPs. (c) Optical image of *M. smegmatis*-treated A549 cells (d) Merged image of the optical (c) and LSCM (a, b) images showing Tre-FSNPs (green) clustered on top of *M. smegmatis* (red).

This selective interaction with *M. smegmatis* over mammalian cells was absent in Glc-NPs where the nanoparticles showed high interactions with both *M. smegmatis* and mammalian cells. The general strategy of using trehalose-facilitated interactions with mycobacteria has high potential in developing effective therapeutic and diagnostic tools for treating mycobacterial infections such as TB.

This work was supported by NIH (R01GM080295 and R21AI109896), and a startup fund from University of Massachusetts Lowell. The authors thank Mr. Christopher Santeufemio for his assistance in the preparation of TEM thin section samples.

Notes and references

- 1 World Health Organization 2014, Geneva, Switzerland.
- 2 M. M. Mehanna, S. M. Mohyeldin and N. A. Elgindy, *J. Control. Release*, 2014, **187**, 183-197.
- 3 M. Daffe and G. Etienne, *Tuber. Lung. Dis.*, 1999, **79**, 153-169.
- 4 P. A. Lambert, *J. Appl. Microbiol.*, 2002, **92**, 46S-54S.
- 5 A. Z. Wang, R. Langer and O. C. Farokhzad, *Annu. Rev. Med.*, 2012, **63**, 185-198.
- 6 R. A. Petros and S. J. M. De, *Nat. Rev. Drug Discovery*, 2010, **9**, 615-627.
- 7 Y. Li, K. Hindi, K. M. Watts, J. B. Taylor, K. Zhang, Z. Li, D. A. Hunstad, C. L. Cannon, W. J. Youngs and K. L. Wooley, *Chem. Commun.*, 2010, **46**, 121-123.
- 8 M. E. Davis, Z. Chen and D. M. Shin, *Nat. Rev. Drug Discovery*, 2008, **7**, 771-782.

- 9 I. Canton and G. Battaglia, *Chem. Soc. Rev.*, 2012, **41**, 2718-2739.
- 10 D. Walczyk, F. B. Bombelli, M. P. Monopoli, I. Lynch and K. A. Dawson, *J. Am. Chem. Soc.*, 2010, **132**, 5761-5768.
- 11 M. Wang and M. Thanou, *Pharmacol. Res.*, 2010, **62**, 90-99.
- 12 T. G. A. Lonhienne, E. Sagulenko, R. I. Webb, K.-C. Lee, J. Franke, D. P. Devos, A. Nouwens, B. J. Carroll and J. A. Fuersta, *Proc. Natl. Acad. Sci. U. S. A.*, 2010, **107**, 12883-12888.
- 13 J. A. Kloepper, R. E. Mielke and J. L. Nadeau, *Appl. Environ. Microbiol.*, 2005, **71**, 2548-2557.
- 14 A. Kumar, A. K. Pandey, S. S. Singh, R. Shanker and A. Dhawan, *Cytometry A*, 2011, **79A**, 707-712.
- 15 A. D. Elbein and M. Mitchell, *J. Bacteriol.*, 1973, **113**, 863-873.
- 16 P. J. Woodruff, B. L. Carlson, B. Siridechadilok, M. R. Pratt, R. H. Senaratne, J. D. Mougous, L. W. Riley, S. J. Williams and C. R. Bertozzi, *J. Biol. Chem.*, 2004, **279**, 28835-28843.
- 17 C. Hoffmann, A. Leis, M. Niederweis, J. M. Plitzko and H. Engelhardt, *Proc. Natl. Acad. Sci. U. S. A.*, 2008, **105**, 3963-3967.
- 18 H. Yamagami, T. Matsumoto, N. Fujiwara, T. Arakawa, K. Kaneda, I. Yano and K. Kobayashi, *Infect. Immun.*, 2001, **69**, 810-815.
- 19 R. Kalscheuer, B. Weinrick, U. Veeraraghavan, G. S. Besra and W. R. Jacobs, *Proc. Natl. Acad. Sci. U. S. A.*, 2010, **107**, 21761-21766.
- 20 A. Nobre, S. Alarico, A. Maranhã, V. Mendes and N. Empadinhas, *Microbiology*, 2014, **160**, 1547-1570.
- 21 K. M. Backus, H. I. Boshoff, C. S. Barry, O. Boutureira, M. K. Patel, F. D'Hooze, S. S. Lee, L. E. Via, K. Tahlan, C. E. Barry, III and B. G. Davis, *Nat. Chem. Biol.*, 2011, **7**, 228-235.
- 22 H. S. N. Jayawardena, K. W. Jayawardana, X. Chen and M. Yan, *Chem. Commun.*, 2013, **49**, 3034-3036.
- 23 X. Wang, O. Ramstrom and M. Yan, *Analyst*, 2011, **136**, 4174-4178.
- 24 X. Wang, O. Ramstrom and M. Yan, *Chem. Commun.*, 2011, **47**, 4261-4263.
- 25 J. P. Gann and M. Yan, *Langmuir*, 2008, **24**, 5319-5323.
- 26 X. Chen, O. Ramstrom and M. Yan, *Nano Res.*, 2014, **7**, 1381-1403.
- 27 L.-H. Liu and M. Yan, *Acc. Chem. Res.*, 2010, **43**, 1434-1443.
- 28 J. Park and M. Yan, *Acc. Chem. Res.*, 2013, **46**, 181-189.
- 29 X. Wang, O. Ramstroem and M. Yan, *Adv. Mater. (Weinheim, Ger.)*, 2010, **22**, 1946-1953.
- 30 X. Wang, L.-H. Liu, O. Ramstrom and M. Yan, *Exp. Biol. Med. (Maywood, NJ, U. S.)*, 2009, **234**, 1128-1139.
- 31 X. Wang, E. Matei, L. Deng, L. Koharudin, A. M. Gronenborn, O. Ramstrom and M. Yan, *Biosens. Bioelectron.*, 2013, **47**, 258-264.
- 32 H. Wang, L.-L. Li, Q. Tong and M.-D. Yan, *ACS Appl. Mater. Interfaces*, 2011, **3**, 3463-3471.
- 33 Q. Tong, X. Wang, H. Wang, T. Kubo and M. Yan, *Anal. Chem.*, 2012, **84**, 3049-3052.
- 34 H. Wang, J. Ren, A. Hlaing and M. Yan, *J. Colloid Interface Sci.*, 2011, **354**, 160-167.
- 35 L.-H. Liu, H. Dietsch, P. Schurtenberger and M. Yan, *Bioconjugate Chem.*, 2009, **20**, 1349-1355.
- 36 C. Xu, K. M. A. Uddin, X. Shen, H. Surangi, N. Jayawardena, M. Yan and L. Ye, *ACS Appl. Mater. Interfaces*, 2013, **5**, 5208-5213.
- 37 X. Wang, E. Matei, A. M. Gronenborn, O. Ramstrom and M. Yan, *Anal. Chem. (Washington, DC, U. S.)*, 2012, **84**, 4248-4252.
- 38 X. Wang, E. Matei, L. Deng, O. Ramstroem, A. M. Gronenborn and M. Yan, *Chem. Commun. (Cambridge, U. K.)*, 2011, **47**, 8620-8622.
- 39 N. Ofer, M. Wishkautzan, M. Meijler, Y. Wang, A. Speer, M. Niederweis and E. Gur, *Appl. Environ. Microbiol.*, 2012, **78**, 7483-7486.
- 40 M. U. Shiloh and P. A. DiGiuseppe Champion, *Curr. Opin. Microbiol.*, 2010, **13**, 86-92.
- 41 N. Fujiwara, T. Naka, M. Ogawa, R. Yamamoto, H. Ogura and H. Taniguchi, *Tuberculosis*, 2012, **92**, 187-192.
- 42 F. Titgemeyer, J. Amon, S. Parche, M. Mahfoud, J. Bail, M. Schlicht, N. Rehm, D. Hillmann, J. Stephan, B. Walter, A. Burkovski and M. Niederweis, *J. Bacteriol.*, 2007, **189**, 5903-5915.
- 43 J. Jin, J.-Y. Zhang, N. Guo, H. Sheng, L. Li, J.-C. Liang, X.-L. Wang, Y. Li, M.-Y. Liu, X.-P. Wu and L. Yu, *Molecules*, 2010, **15**, 7750-7762.
- 44 L. Rodrigues, J. Ramos, I. Couto, L. Amaral and M. Viveiros, *BMC Microbiol.*, 2011, **11**, 35.
- 45 P. Lu, H. Lill, D. Bald, C. Villellas, A. Koul and K. Andries, *J. Antibiot.*, 2014.
- 46 M. Liong, J. Lu, M. Kovichich, T. Xia, S. G. Ruehm, A. E. Nel, F. Tamanoi and J. I. Zink, *ACS Nano*, 2008, **2**, 889-896.